A PRELIMINARY STUDY OF A NEW DEVICE FOR PRODUCING HIGH-ENTHALPY, SHORT-DURATION GAS FLOWS

By Robert L. Trimpi

NASA Langley Research Center
Langley Air Force Base, Va.

For presentation at the Second National Hypervelocity Techniques Symposium

Denver, Colorado
March 19-20, 1962

A PRELIMINARY STUDY OF A NEW DEVICE FOR PRODUCING HIGH-ENTHALPY, SHORT-DURATION GAS FLOWS

By Robert L. Trimpi*

For presentation at the Second National
Hypervelocity Techniques Symposium

SUMMARY

A preliminary investigation is presented of the expansion tube, a new device utilizing both unsteady shock waves and expansion waves to produce short-duration, high-enthalpy hypersonic airflows. The unsteady expansion processes therein result in a large total enthalpy multiplication. A real air analysis assuming idealized diaphragm bursts, centered expansion waves, and an equilibrium continuum flow showed that the expansion tube test-section velocity would exceed that of a comparable shock tunnel by factors greater than two for the same ambient density and pressure. The possibility of equilibrium flow in the test section appears favorable since the maximum dissociation in the expansion tube cycle is low. The required driver pressures are relatively low and are within present-day state of the art for duplication of the lunar reentry trajectory. A quick look at some preliminary experimental results is briefly reported and appears encouraging, although there are many known and anticipated advantages and disadvantages of this concept which require further study.

SYMBOLS

a	velocity of sound, ft/sec
H	total enthalpy
h	local enthalpy
l_D	length of driver section of expansion tube
l_{S_1}	length of driven section of expansion tube
l_{S_2}	length of expansion section of expansion tube

*Head, Reentry Physics Branch, Langley Research Center, NASA.

M	flow Mach number
M_{S_1}	Mach number of primary shock wave
M_{S_2}	Mach number of secondary shock wave
p	absolute pressure
S_1	primary shock wave
S_2	secondary shock wave
s	entropy per unit mass
T	absolute temperature
t	time
Δt	nominal testing time (time between passage of entropy discontinuity and arrival of expansion fan at test section)
U_{S_2}	velocity of secondary shock wave
u	velocity of fluid
$W/C_D A$	ballistic parameter, lb/sq ft
Z	compressibility factor, $p/\rho RT$
ξ	distance from shock wave to entropy discontinuity

Subscripts:

o	standard conditions
1,2,3,4	conditions in expansion tube (fig. 3) and corresponding conditions in shock tunnel
5	test-section conditions
10,20	conditions in expansion tube (fig. 3)

INTRODUCTION

The problem which faces an experimentalist who tries to attain a flow which duplicates the ambient conditions at various altitudes for a given velocity may be obtained by inspecting figure 1. On this altitude-velocity map is cross plotted the stagnation conditions required for an equilibrium isentropic expansion to produce the velocities indicated at the ambient conditions of the various altitudes. Extrapolations of existing Mollier diagrams have been made so that this is only an approximate plot. Note that the pressures vary from 10^4 to over 10^6 atmospheres, the temperatures vary from 20,000° to 30,000° K, and the compressibility factor (Z) varies from 1.4 to approximately 2. The heavy dots are the 10g undershoot trajectory of a nonlifting lunar reentry vehicle with a ballistic parameter $\frac{W}{C_D A}$ of 50 pounds per square foot. Since the maximum heating occurs near the knee of the curve, duplication would require stagnation pressures above a million atmospheres, stagnation temperatures greater than 25,000° K, and a value of Z of approximately $1\frac{1}{2}$. The power requirements (i.e., the energy flowing past the test section) would be in excess of 15 megawatts per square foot. Also shown is the design performance curve of the Cornell Aeronautical Laboratory shock tunnel (ref. 1). This heated hydrogen-drive tunnel, which is illustrative of operational design shock tunnels at present, has a potential far below that required for study of the lunar return or higher velocities.

It appears that some device is needed which does not require attainment of the stagnation conditions in a part of its cycle (due to high stagnation pressures and temperatures) and which also operates for only a very short time (due to the tremendous power requirements). One solution to the problem of attaining high enthalpy and still avoiding the stagnation state may be found in a device using unsteady expansion waves. A comparison of the differential velocity increase and total enthalpy change in a steady and unsteady isentropic expansion are shown in figure 2. On the left are the relations for the steady expansion in which a given velocity change du is equal to $-1/u$ times the local enthalpy increase dh, and the total enthalpy H is constant. In the unsteady expansion on the right (an upstream expansion is considered here) du is equal to $-dh/a$. Notice the a in the denominator contrasted to the u in the steady expansion and also the total enthalpy differential is equal to $-(M - 1)$ times the local enthalpy change. Consequently, for a facility which requires high velocities and high Mach number there is much to be gained with an unsteady expansion because for a given enthalpy decrease the velocity increment is a factor $M = u/a$ higher than the steady expansion. Furthermore, the total energy is increased in the expansion wave. This is not a violation of

the conservation of energy if one integrates throughout the whole unsteady flow.

DESCRIPTION OF EXPANSION TUBE

A facility utilizing such an unsteady expansion wave has been designed and designated as an "Expansion Tube." The next figure is a distance time plot of the cycle for this expansion tube. The tube is comprised of three sections: the driver section, driven section, and expansion section. Diaphragms separate the driver section and the expansion section from the driven section. Initial pressures decrease by orders of magnitude progressively from one section to the next. The operating cycle is as follows: The primary diaphragm ruptures so that a shock S_1 is propagated from the driver gas (4) into the test gas (1) heating and accelerating the test gas. This shock progresses through the test gas and strikes the diaphragm separating the test gas from the accelerating gas (10) whereupon this diaphragm bursts and a new shock wave S_2 propagates into the accelerating gas. Concurrently, an upstream expansion wave is formed, progressing back into the test gas. Since the flow (2) is supersonic, however, the expansion wave is washed downstream. This expansion accelerates the test gas from the state (2) to the state (5), and at the same time causes a decrease in temperature and pressure. Consequently, in state (5) we now have gas at a very high velocity which has been accelerated by two processes, one a shock and one an expansion. The ambient conditions in (5) are at a low temperature and pressure because the expansion wave reduced the temperature and pressure from the high values in (2) behind the shock wave. The expansion fan is the key to the successful operation of such a tube.

Figure 4 shows the total enthalpy multiplication across the expansion fan, i.e., the ratio of the total enthalpy in the region (5) to the total enthalpy after the shock wave in region (2). Values of this enthalpy ratio are 4 and above for real air. Consequently, over 80 percent of the energy of the flow is added in the expansion fan.

A comparison between the theoretical performance of the expansion tube and nonreflected shock tunnel appears on figure 5. The ordinate is the primary shock Mach number (M_{S_1}) and the abscissa is the test-section Mach number (M_5). For the expansion tube, curves are drawn for real air at various altitudes and for perfect air at two temperature ratios a_5/a_1.

Only the real air curves are shown for the nonreflected shock tunnel. The expansion tube, by virtue of its energy multiplication in the expansion fan, can produce test-section Mach numbers from 2 to $2\frac{1}{2}$ times those which would be attainable in a nonreflected shock tunnel for the same primary shock Mach number. (For a high-temperature driver at the same driver pressure, a real air reflected shock tunnel is slightly lower in performance in regard to velocity and altitude simulation than a nonreflected shock tunnel. It may also be noted that for real air the enthalpy multiplication behind a reflected shock is up to about 20 percent.)

THERMODYNAMIC STATES IN EXPANSION TUBE

The various states occurring in the expansion tube cycle will now be examined. First, consider the pressure initially in the accelerating chamber (p_{10}). In order to maximize this low pressure, a "light gas" (low molecular weight) will be utilized; and if helium is used for this purpose, the pressures required in the accelerating chamber will be those of figure 6. Test-section Mach number is the abscissa and accelerating chamber pressure the ordinate. The lunar trajectory requires pressures from 0.05 micron to better than 10 microns; such pressures are easily attainable with reasonable care in vacuum practices.

Next, consider the conditions behind the primary shock, state 2. The pressures are not shown here because they are covered in an NASA report (ref. 2). However, these pressures are moderate, and for the lunar return have a maximum of about 750 psi. The compressibility behind the shock wave is shown on the next figure. Note the low value of Z_2 with a maximum of about 7 percent dissociation $(Z_2 - 1)$ for the lunar trajectory. This value is in contrast to the 50 percent for a stagnation-type facility (fig. 1).

Finally, consider the driver pressures. The case of a helium driver gas heated either by an arc or by combustion processes has already been treated in reference 2. Here we will treat a hydrogen gas driver moderately heated to 550° K. See figure 8. The lunar return theoretically requires only a driver pressure of a thousand atmospheres. Attenuation may increase this by a factor of 2 or 3, but the resultant pressure levels are still within the state of the art.

LENGTHS OF COMPONENT SECTIONS

The lengths of the various component sections are determined by choosing the lengths so that the wave reflected from the closed end of the driver will intersect the leading edge of the expansion fan at the same point that the entropy discontinuity separating the driver and driven gas intersects the expansion fan. See figure 9. The testing time, designated Δt on this figure, is the time between the arrival of the test gas at the test section and the arrival of the trailing edge of the expansion fan.

The value of the testing time per foot of expansion chamber is plotted against test-section Mach number in figure 10. The testing time per foot decreases as the Mach number increases and is approximately proportional to $1/M^2$. Since the testing times are very small, of the order of a microsecond per foot, long accelerator chamber lengths will be required to have appreciable testing time. However, for radiation studies, testing times of the order of from a fraction up to 10 microseconds are adequate. For comparison purposes, a nonreflected shock tunnel having a driven length equal to the expansion chamber length would have test time about twice that of an expansion tube, and a reflected tailored shock tunnel would have a testing time 20 times that of the expansion tube. The foregoing comparison neglects the starting time of the nozzles of the shock tunnels, and if this starting time is considered, the ratios will be markedly reduced. The incident shock-wave tubes such as Avco (ref. 3) has used to study the nonequilibrium radiation would also have testing times up to about twice that of the expansion tube of equivalent major section lengths.

The ratio of driven chamber to expansion chamber length l_{S_1}/l_{S_2} is plotted against test-section Mach number in the next figure. The length of the driven section l_{S_1} is several orders of magnitude less than the length of the expansion chamber. For Mach numbers above 30, the driven length is less than 1 percent of the expansion tube length.

The driver length is, of course, a function of the driver gas and its temperature. Hydrogen at 550° K is the gas treated herein, and the ratio of the driver length to the expansion chamber length l_D/l_{S_2} is plotted in figure 12. This ratio varies from less than 1 percent down to a fraction of a percent. It might be noted that the ratio of the driver to driven sections l_D/l_{S_1} is less than one-fourth for the hydrogen driver.

SOME PRACTICAL PROBLEMS OF THE EXPANSION TUBE

So far the analysis has assumed a real but inviscid gas and that diaphragm bursts may be represented by instantaneous removal of the diaphragms. Practically, however, the problem of diaphragm burst and shock formation must be considered. These problems will necessitate longer driver and driven sections than theoretically required. The effect of the nonideal rupture of the secondary diaphragm is not known at this time.

Damage to the model from diaphragm particles striking the model surface is another problem. Relief from this damage might be obtained by employing a curved expansion chamber which would act as a centrifuge for the heavier diaphragm particles.

Viscous effects must also be considered. The long length of low Reynolds number flow will result in large boundary-layer thicknesses, so that a type of "pipe flow" may result if the boundary layer is thick enough to join the one from the opposite wall. The helium flow behind the secondary shock is at a very low Reynolds number since the gas is very hot and at low pressure. Consequently, there will be a strong wall interaction. The leaky piston concept introduced by Duff and Anderson (refs. 4 and 5) which has been used to explain the performance of low-density shock tubes is applicable here also. This concept is schematically illustrated in figure 13. The high cooling of the wall results in a large negative value for the boundary-layer displacement thickness in the region 20 so that, at a short distance behind the shock, all the fluid which passed through the shock is in the boundary layer, and the entropy discontinuity and shock wave move at the same speed. In order to estimate the distance at which the boundary displacement thickness is equal to minus the half height of a two-dimensional channel (or radius if axisymmetrical) N. B. Cohen of the Langley Laboratory has obtained a few boundary-layer solutions on the digital computer for two-dimensional laminar flow of helium. A typical result of these solutions for an expansion tube height (diameter) of 1 foot and a velocity U_5 of 36,000 ft/sec is that ξ is approximately 3/4 of an inch when $p_{10} \approx 1$ micron mercury. The time for the flow contained in region of length ξ to pass a fixed station on the wall is approximately $1\frac{1}{4}$ microseconds. Obviously these solutions are only indicative of the lengths which arise in the problem since they were obtained assuming a constant outer potential flow. There will be a strong interaction between the rapidly growing boundary layer and the outer flow which will invalidate these solutions. However, they do indicate that within very short distances behind the shock S_2 the helium is essentially all contained in a thin boundary layer near the wall.

PRELIMINARY EXPERIMENTS

A very limited exploratory investigation using the Langley Reentry Physics 4-Inch High-Pressure Shock Tube as an expansion tube has been conducted by J. J. Jones, J. A. Moore, J. E. Nealy, and J. E. Gardner. This shock tube was designed for optional use as a buffered-drive shock tube and consequently could easily be converted to an expansion tube by using the buffer chamber as the driven section (fig. 14). The inside diameter of the tube was $3\frac{3}{4}$ inches. The oxygen-hydrogen-helium combustion driver was 14 feet long, the driven chamber approximately $24\frac{1}{2}$ feet long, and the expansion chamber 47 feet long. Models were mounted at the end of the expansion chamber.

At this time the experimental results are inconclusive in many respects because they are limited and were rather hastily obtained. However, one thing was immediately obvious; namely, that the extent of the helium region behind the shock was very limited. Self-luminous high-speed motion pictures taken of the luminous gas cap ahead of various shapes showed that the shock which first appeared was not a shock in helium. This was checked both by measuring the shock detachment distance on blunt bodies and by use of a cone having an included angle of 120° such that the shock in helium would be detached, whereas in air it would be attached. The pictures so obtained conclusively proved that the first recorded radiation did not arise from the gas cap behind shocks in helium.

Ionization gages located along the length of the expansion tube picked up a disturbance so that its position and time, and consequently velocity, could be determined. The extrapolation of this position time curve coincided with the appearance of the radiation at the model. Thus, although it is not known whether the velocity of the helium shock or the velocity of the air-helium discontinuity was measured (since the distance between the two is negligible) it is felt that the velocity measured was the velocity of the airflow. Velocities in excess of 36,000 ft/sec have been obtained. Since most of the shapes studied are classified, they will not be discussed herein. However, one unclassified shape was tested early in the study because of its ready availability. The last figure is a frame from a fastex high-speed motion-picture sequence of a stove bolt at 0° angle of attack in a flow in excess of 30,000 ft/sec. It is of interest to note that the detachment distance is approximately 4 percent of the diameter of the bolt head.

CONCLUSION

In this paper we have examined, in a preliminary manner, a facility which appears to have capability for the generation of high-speed equilibrium airflows at ambient conditions duplicating those of the atmosphere. Several problems have been mentioned, several were not mentioned. Predominant problems are the short testing time, diaphragm bursts, and the viscous effects of the fluid. However, at this stage of the investigation it appears that the expansion tube, theoretically, possesses a tremendous potential. Our preliminary experimental look was encouraging and consequently we believe that a continued theoretical and experimental investigation of this expansion tube or variations thereof is most desirable.

REFERENCES

1. Hertzberg, A., Wittliff, Charles E., and Hall, Gordon J.: Summary of Shock Tunnel Development and Application to Hypersonic Research. Cornell Aeronautical Laboratory, Inc., Report No. AD-1052-A-12, July 1961.

2. Trimpi, Robert L.: A Preliminary Theoretical Study of the Expansion Tube, A New Device for Producing High-Enthalpy Short-Duration Hypersonic Gas Flows. NASA TR 133, 1962.

3. Lin, Shao-Chi and Fyfe, Walter I.: Low-Density Shock Tube for Chemical Kinetic Studies. Avco Everett Research Laboratory, Research Report 91, July 1960.

4. Duff, Russell E.: Shock Tube Performance at Low Initial Pressure. Physics of Fluids, Vol. II, p. 207, 1959.

5. Anderson, G. F.: Shock-Tube Testing Time. Journal of Aero/Space Sciences, Vol. 26, p. 184, 1959.

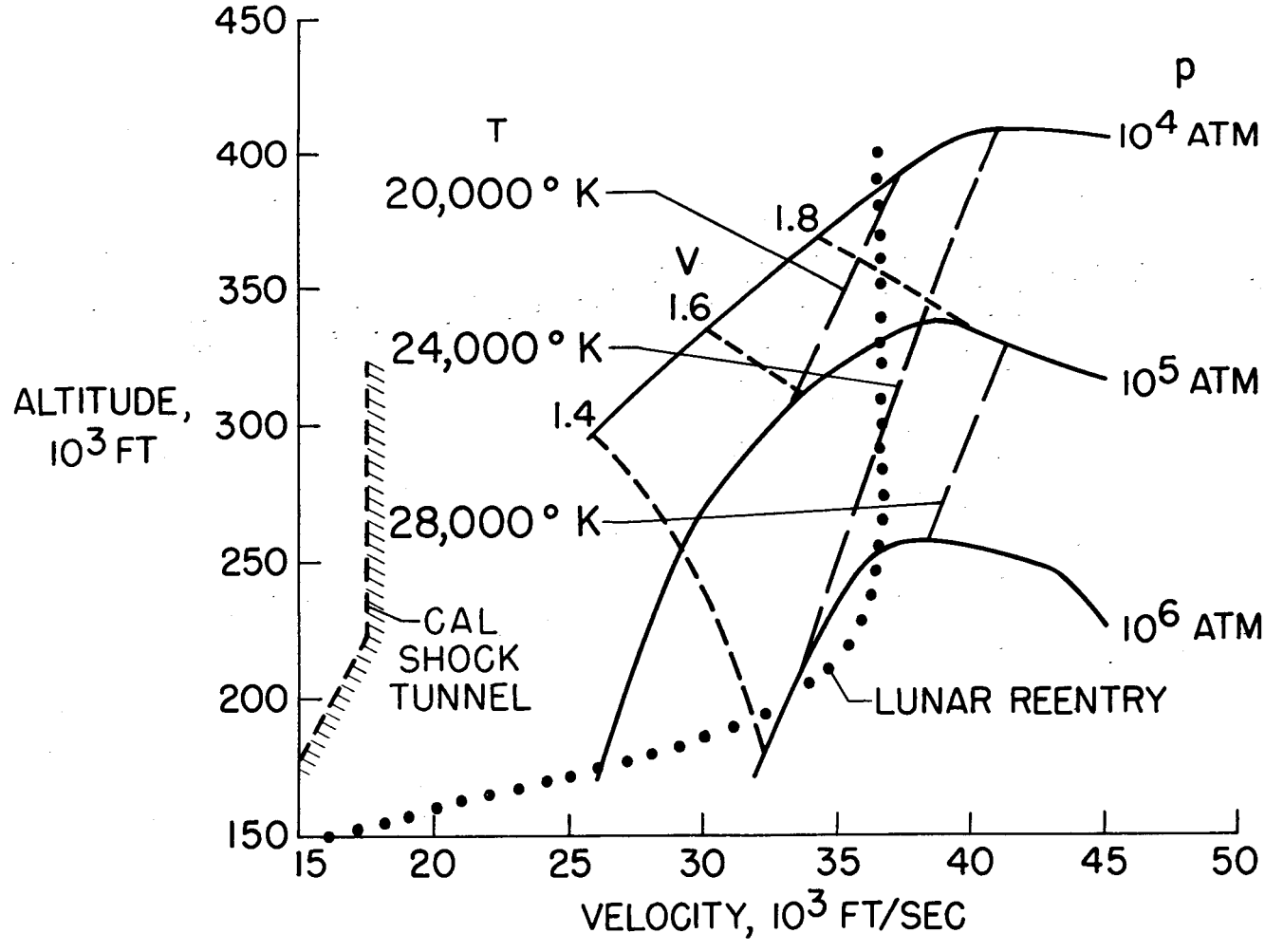

NASA

Figure 1.- Stagnation conditions required for isentropic expansion to duplicate velocities at ambient altitude conditions.

STEADY EXPANSION	UNSTEADY EXPANSION (Q WAVE)
$du = -\left(\frac{dh}{u}\right)_{S/R}$	$du = -\left(\frac{dh}{a}\right)_{S/R}$
$dH = 0$	$dH = -(M-1)\,dh$

NASA

Figure 2.- Comparison between steady and unsteady expansions.

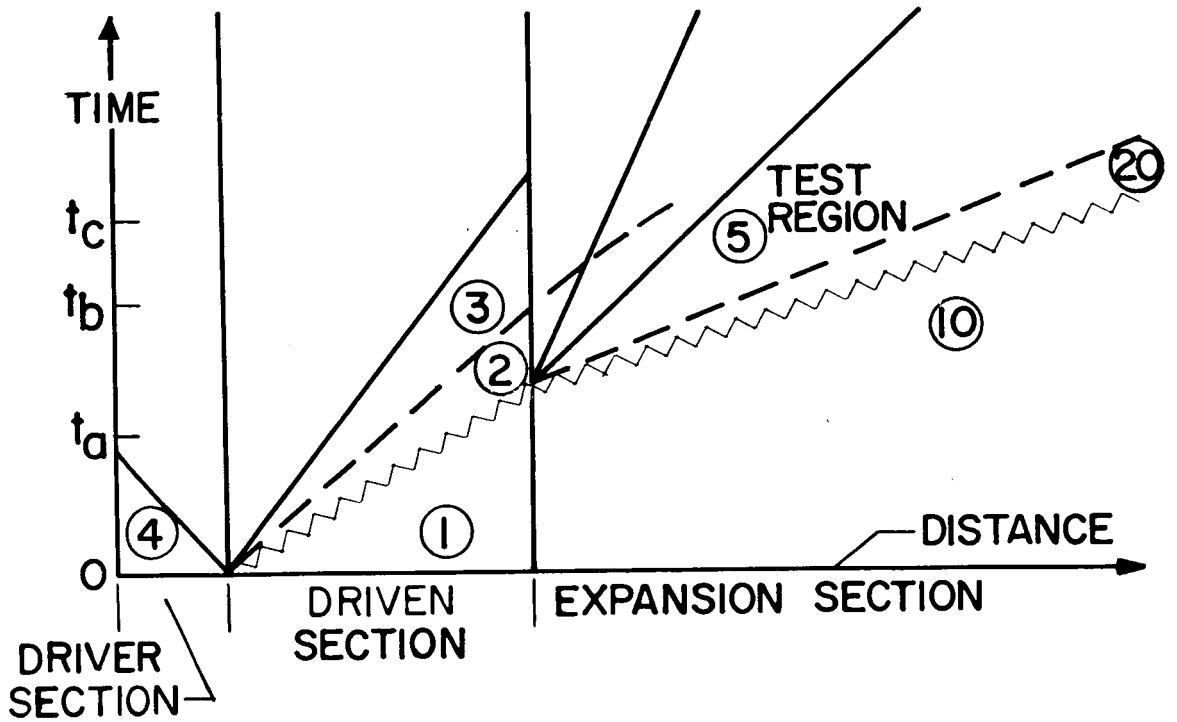

(a) Distance time plot for expansion tube.

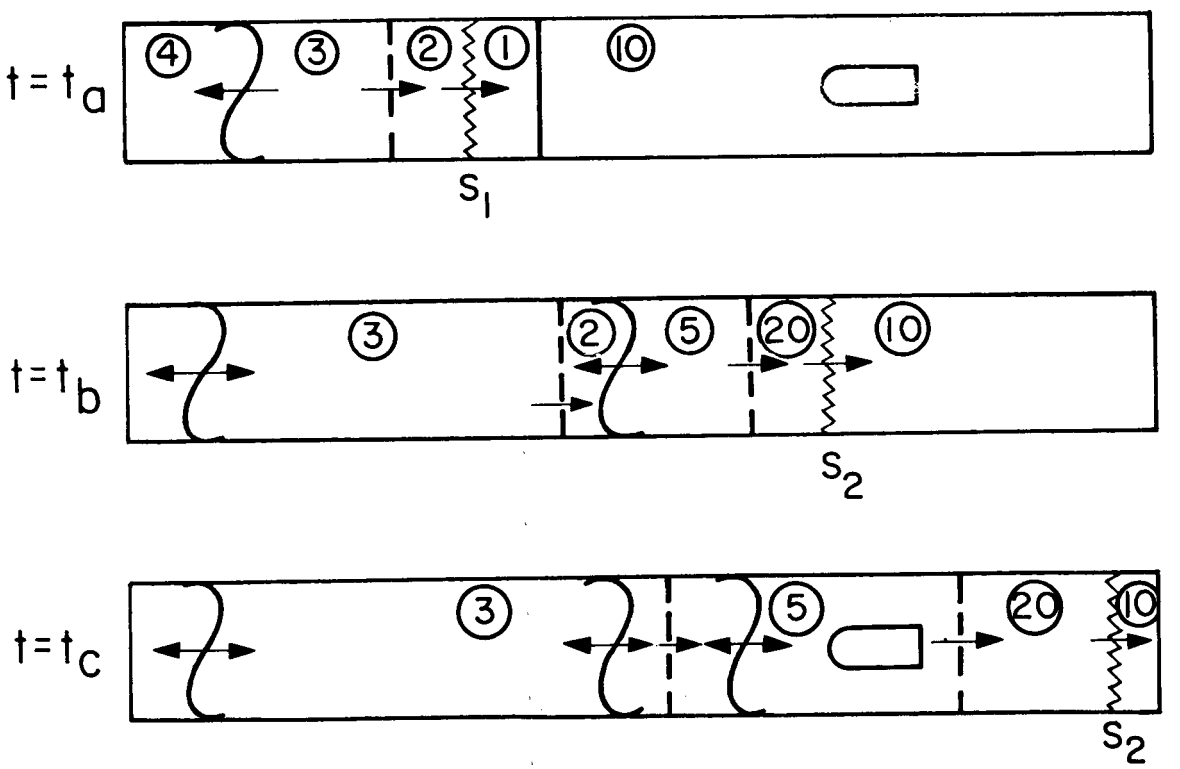

(b) Sketches of expansion tube cycle. NASA

Figure 3.- Expansion tube operation.

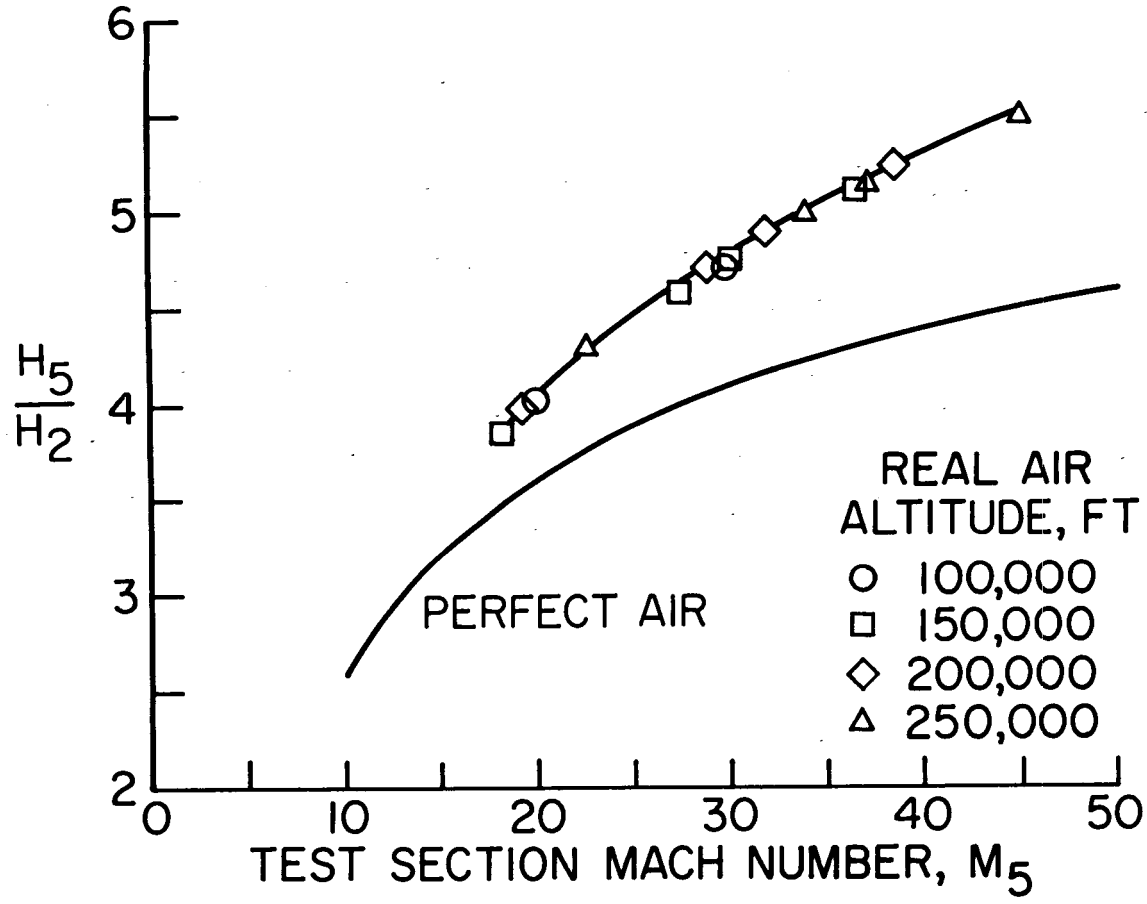

NASA

Figure 4.- Total enthalpy multiplication in expansion fan.

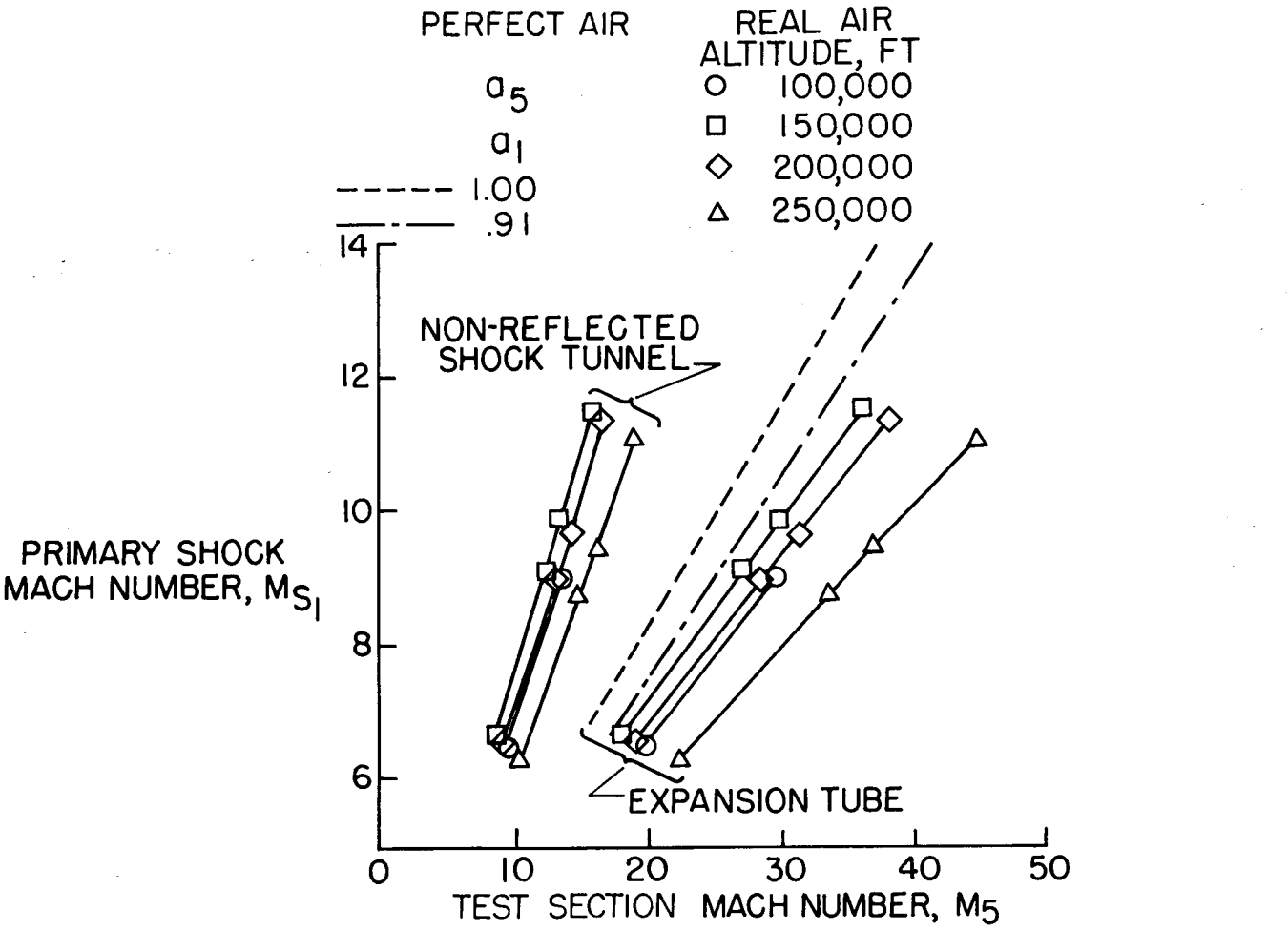

NASA

Figure 5.- Relation between primary shock Mach number and test-section Mach number.

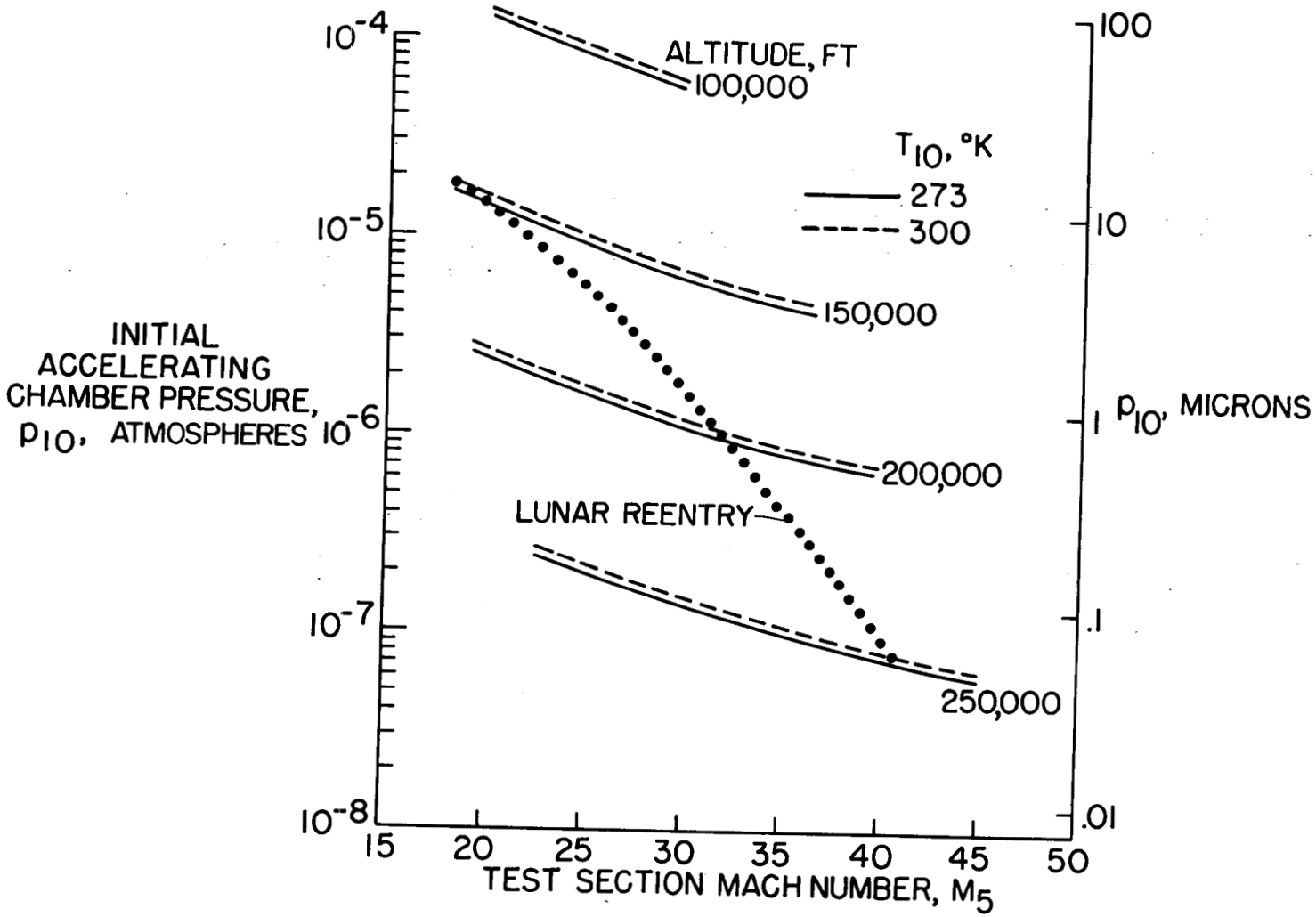

NASA

Figure 6.- Initial helium pressure in accelerating chamber.

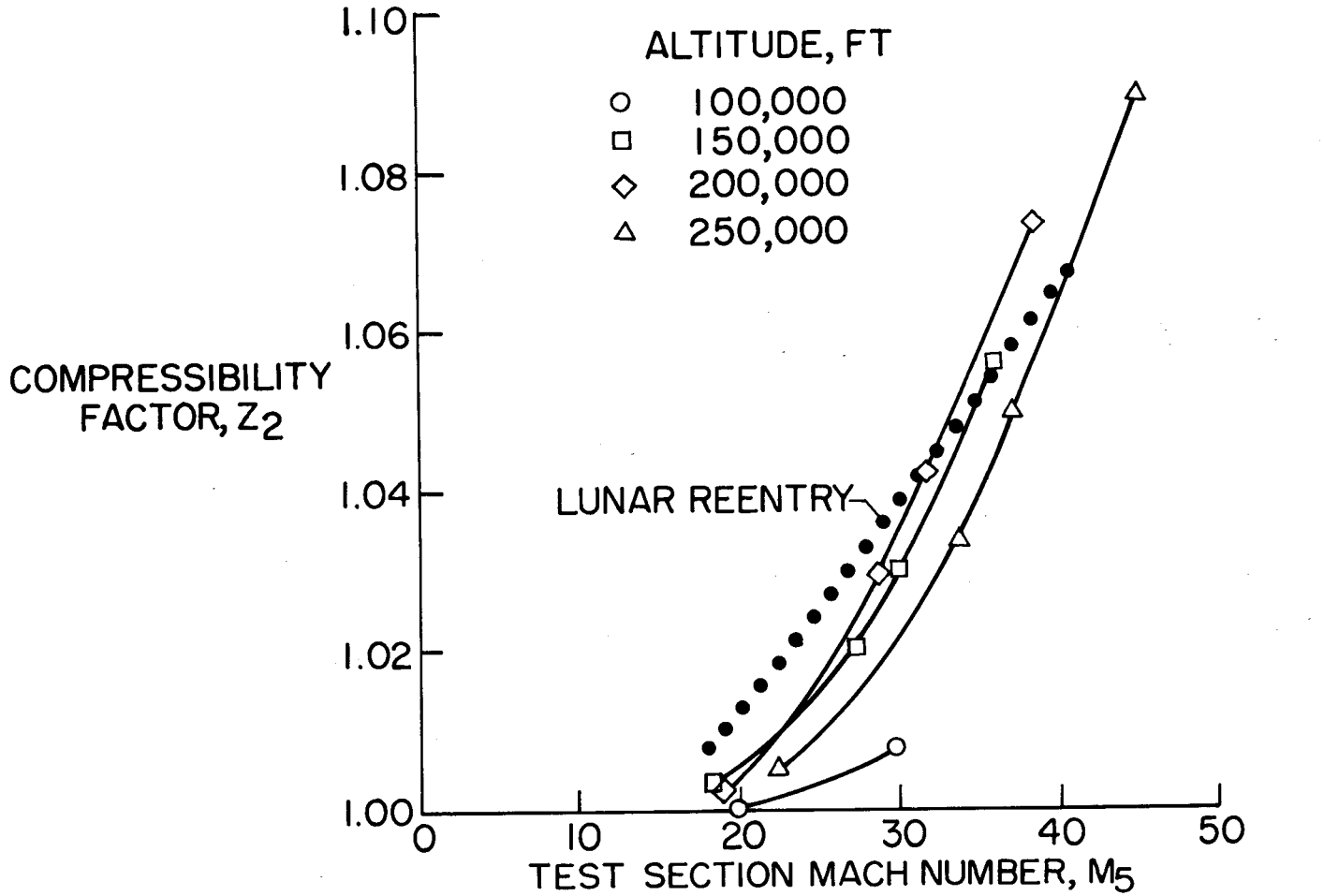

Figure 7.- Compressibility factor behind primary shock wave.

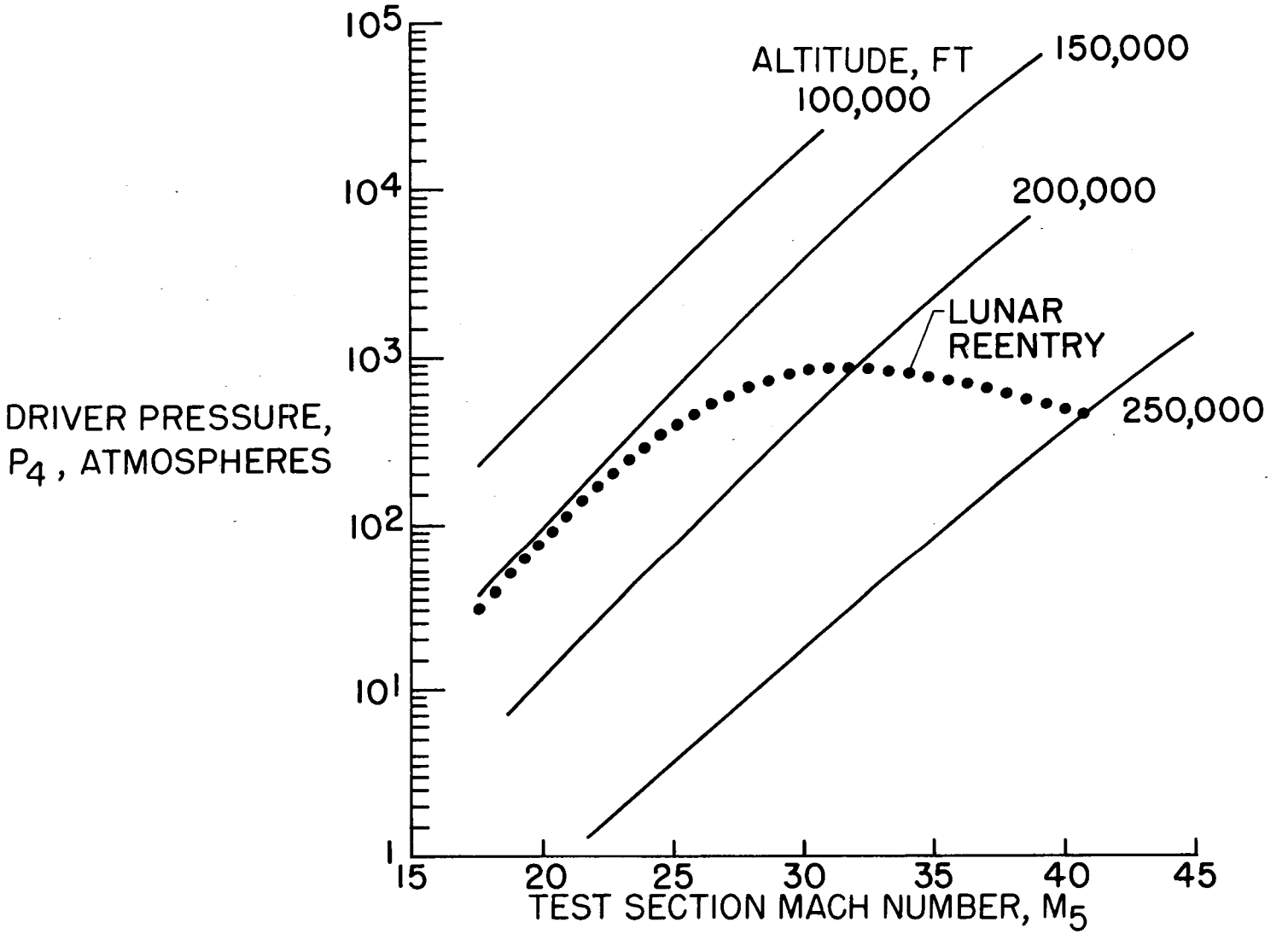

Figure 8.- Driver pressure for hydrogen drive. $T_4 = 550^\circ$ K.

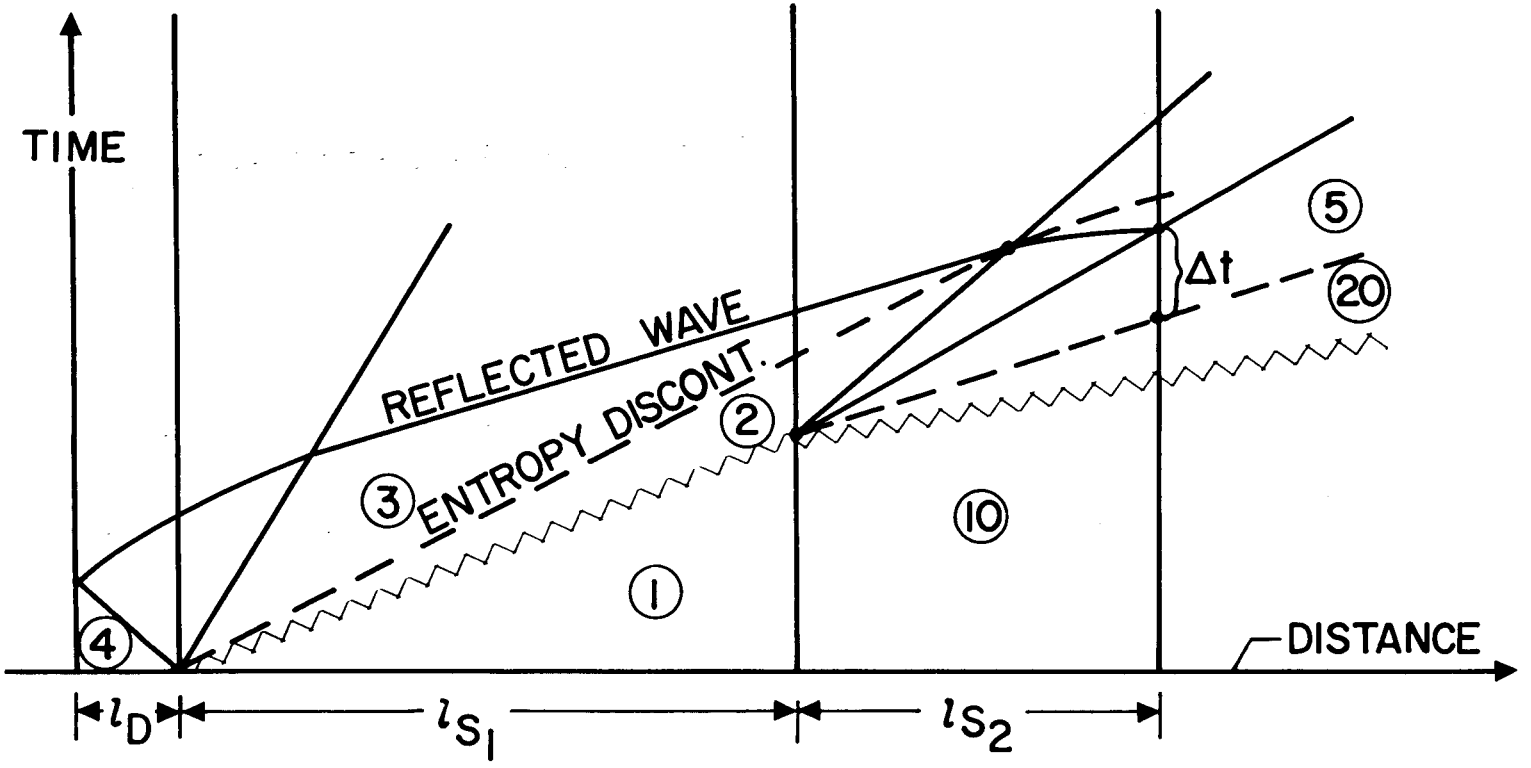

NASA

Figure 9.- Wave diagram to determine section lengths.

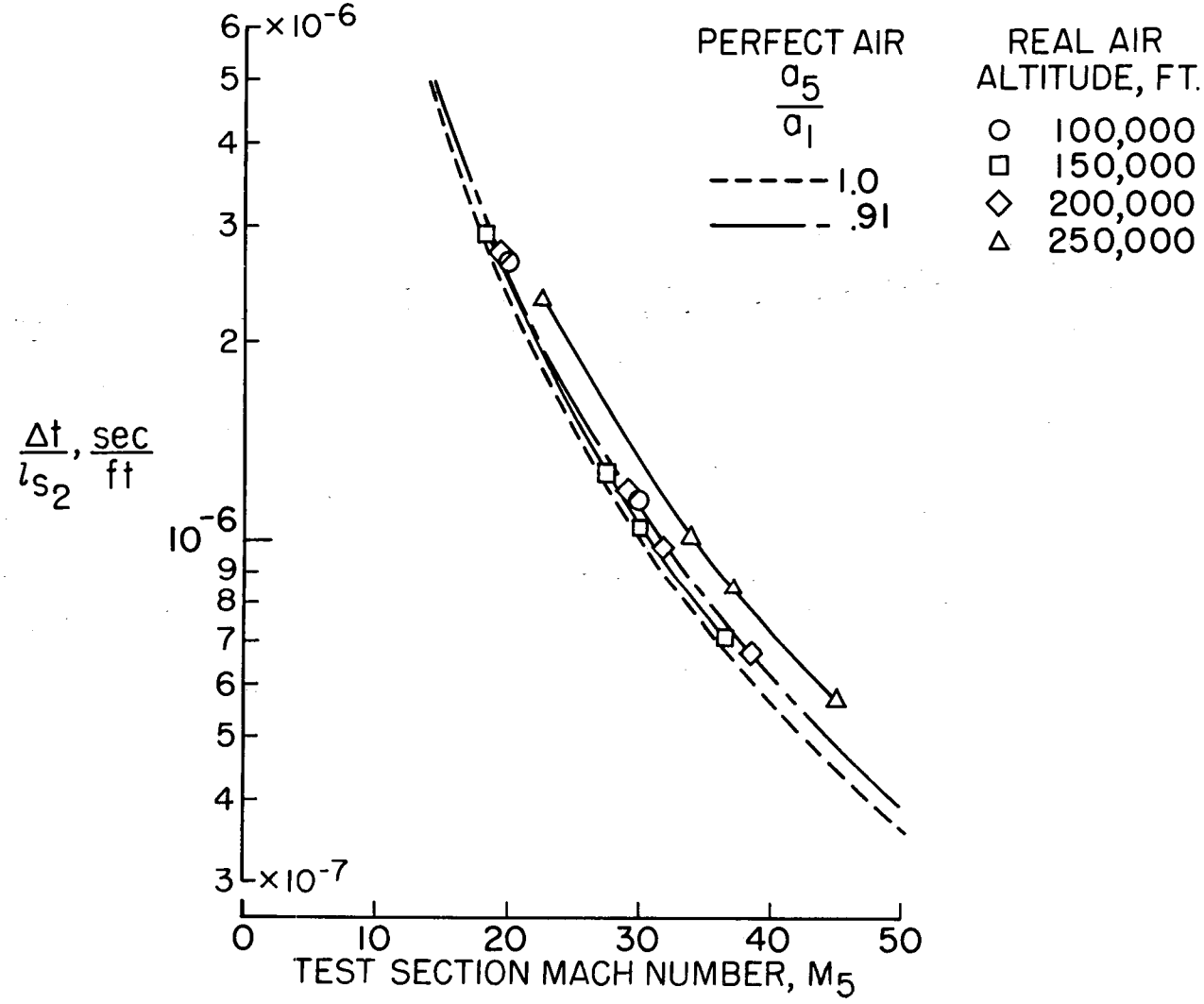

NASA

Figure 10.- Testing time per foot of expansion chamber.

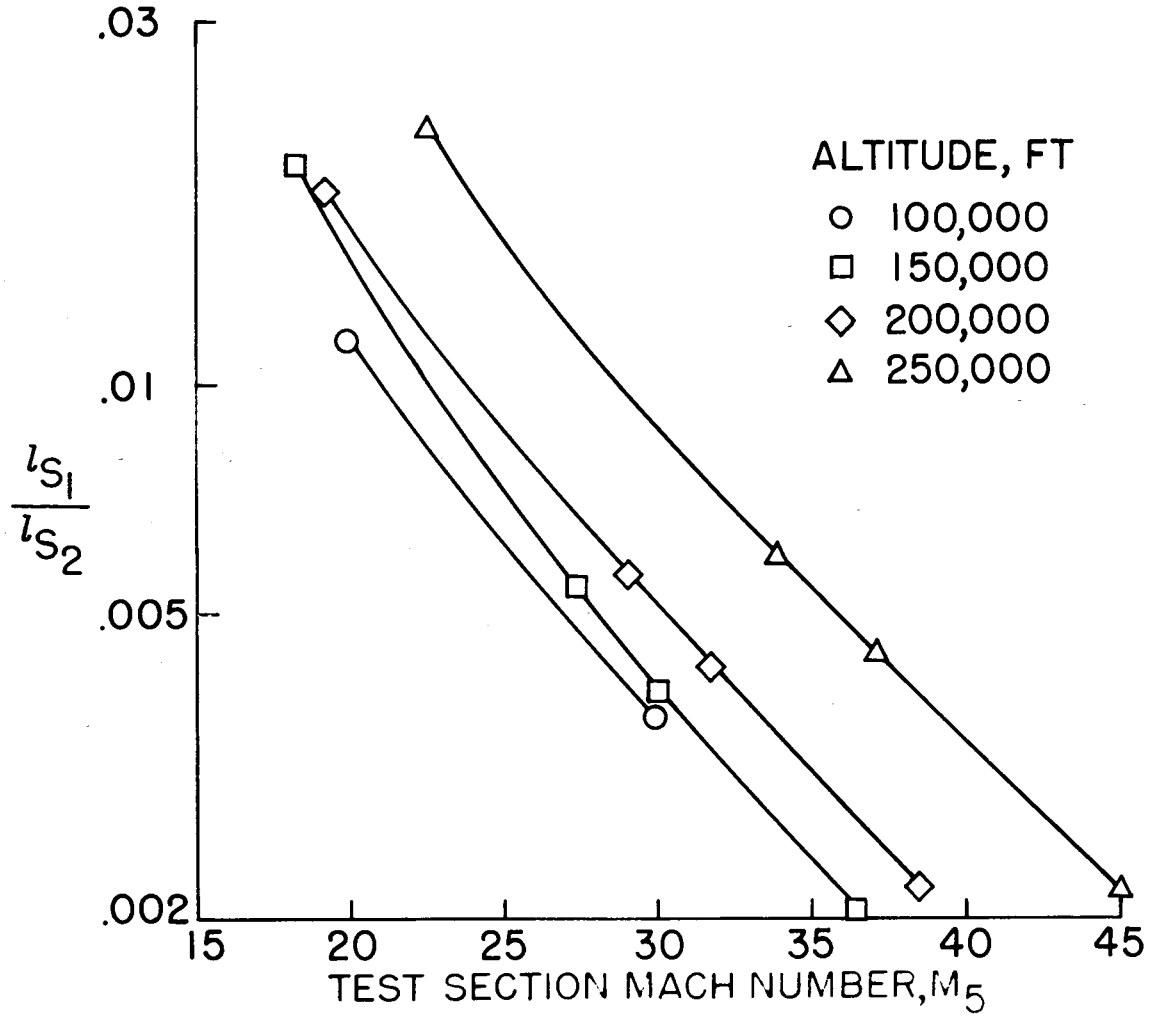

NASA

Figure 11.- Ratio of lengths of driven chamber to expansion chamber.

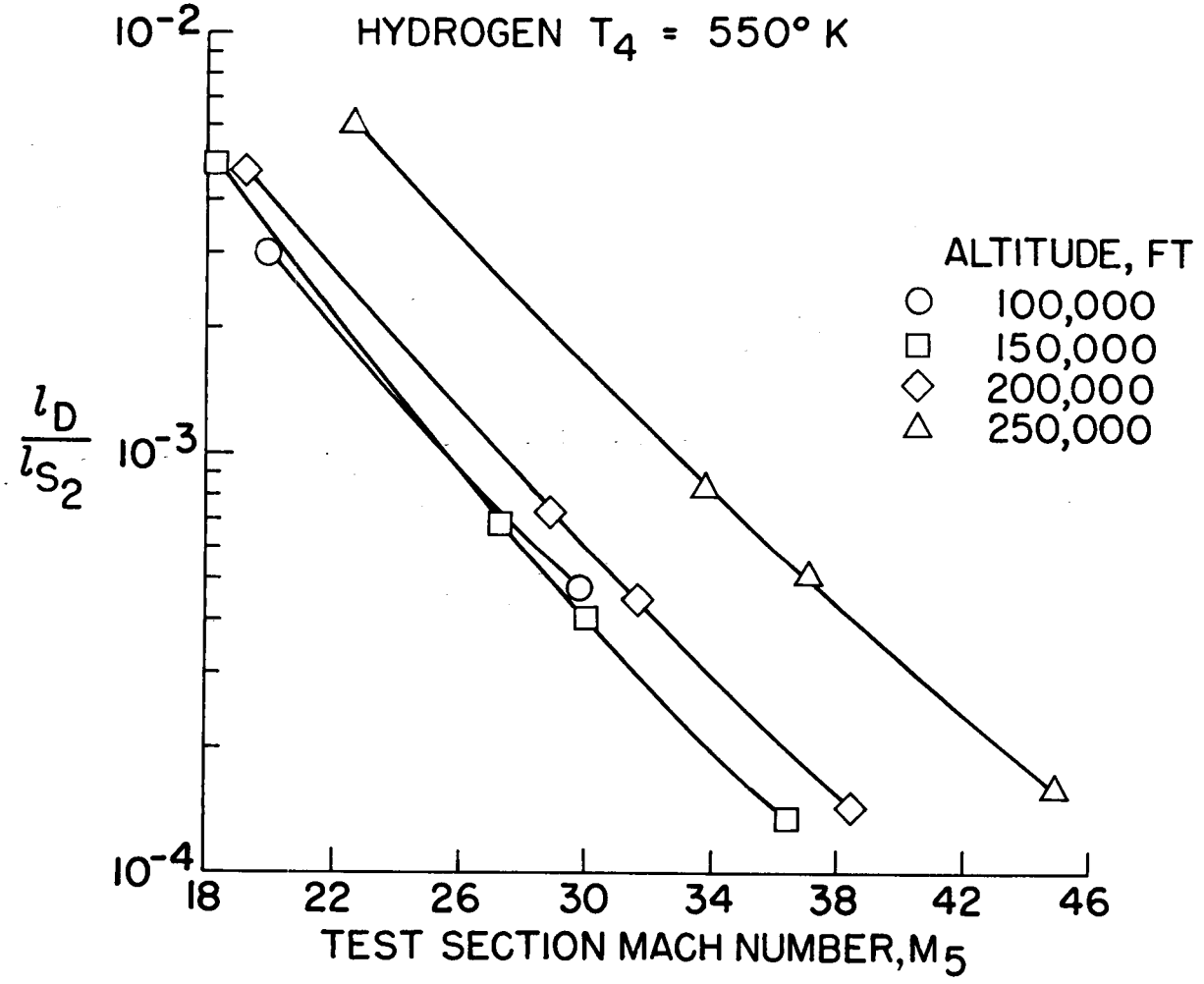

NASA

Figure 12.- Ratio of lengths of driver chamber to expansion chamber.

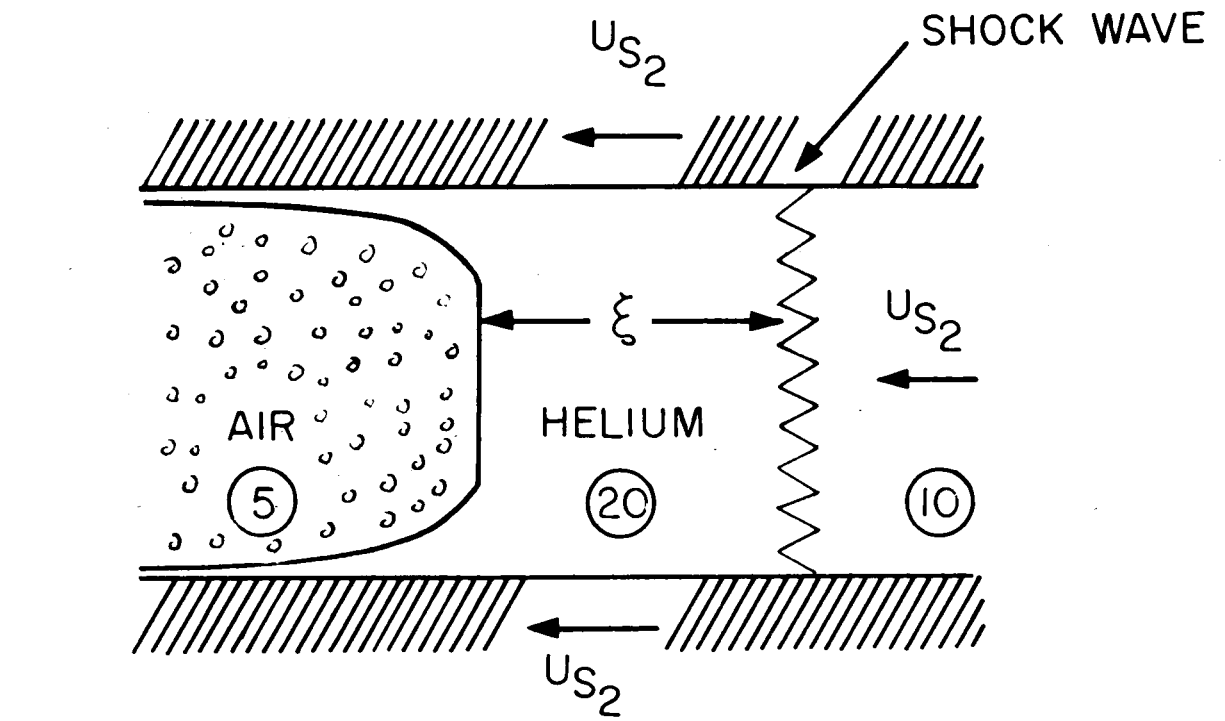

Figure 13.- Leaky piston concept of flow behind shock wave.

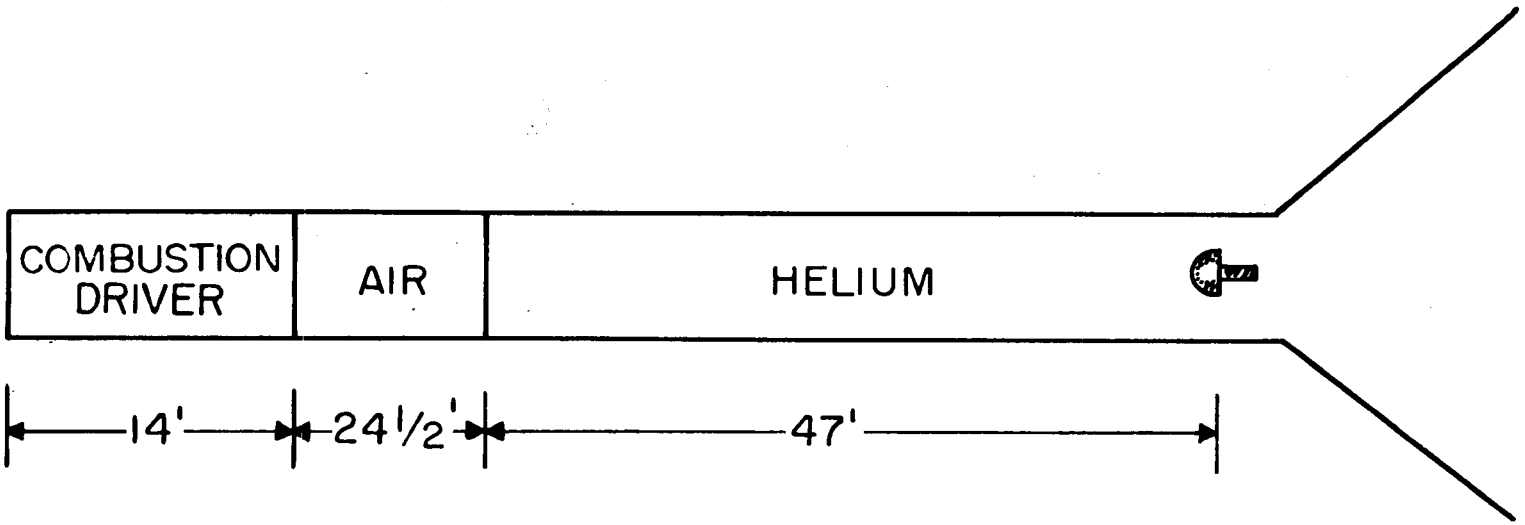

NASA

Figure 14.- 4-inch high pressure shock tube used as expansion tube.

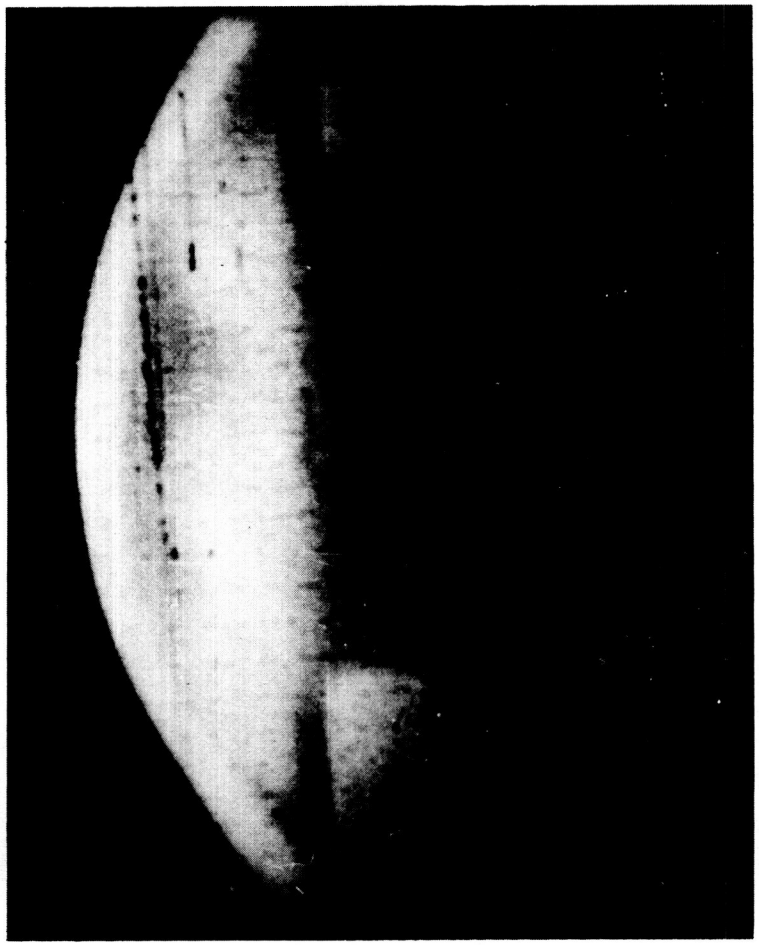

NASA

Figure 15.- Self-luminous picture of stove bolt at 30,000 ft/sec.